

1 Remote sensing reveals fire-driven enhancement of a C₄ rhizomatous 2 alien grass on a small Mediterranean volcanic island

3 Riccardo Guarino^{1*}, Daniele Cerra^{2*}, Renzo Zaia³, Alessandro Chiarucci⁴, Pietro Lo Cascio⁵, Duccio
4 Rocchini⁴, Piero Zannini⁴, Salvatore Pasta⁶

5 ¹Department of Biological, Chemical and Pharmaceutical Sciences and Technologies (STEBICEF), University of Palermo,
6 90123 Palermo, Italy

7 ²Remote Sensing Technology Institute (IMF), German Aerospace Center DLR, 82234 Oberpfaffenhofen, Germany

8 ³Magmatrek, 98050 Stromboli (ME), Italy

9 ⁴BIOME Lab, Department of Biological, Geological and Environmental Sciences, Alma Mater Studiorum, University of
10 Bologna, 40126 Bologna, Italy

11 ⁵NESOS, 98055 Lipari (ME), Italy

12 ⁶Institute of Biosciences and BioResources (IBBR), National Research Council, 90129 Palermo, Italy

13 *These authors contributed equally to this work.

14 **Correspondence:** Riccardo Guarino (riccardo.guarino@unipa.it)

15 **Abstract.** The severity and the extent of a large fire event that occurred on the small volcanic island of Stromboli (Aeolian
16 archipelago, Italy) on 25-26 May 2022 was evaluated through remotely sensed data to assess the short-term effect of fire on
17 local plant communities. For this purpose, the differential Normalised Burned Index (dNBR) was used also to quantify the
18 extent of early-stage vegetation recovery, dominated by *Saccharum biflorum* Forssk. (Poaceae), a rhizomatous C₄ perennial
19 grass of paleotropical origin. The burned area was estimated to have an extension of 337.83 ha, corresponding to 27.7% of the
20 island surface and to 49.8% of Stromboli's vegetated area. On the one hand, this event considerably damaged the native plant
21 communities, hosting many species of high biogeographic interest. On the other hand, *Saccharum biflorum* clearly benefited
22 from fire. In fact, this species showed a very high vegetative performance after burning, being able to exert unchallenged
23 dominance in the early stages of the post-fire succession. Our results confirm the complex and probably synergic impact of
24 different human disturbances (repeated fires, introduction of invasive alien plants) on the natural ecosystems of small volcanic
25 islands.

26 **Keywords.** Biological succession, Disturbance, Satellite imagery, Sprouters, Vegetation dynamics.

27 Introduction

28 Wildfires are a main disturbance factor affecting the Mediterranean terrestrial ecosystems, whose vegetation patterns are
29 largely influenced by interactions with fire. Fire frequency and severity delineates landscape attributes (Pausas, 2006; Jouffroy-
30 Bapicot et al., 2021), affects the structure and composition of the vegetation (Trabaud, 1994) and regulates speed and direction
31 of ecological succession dynamics (Canelles et al., 2019). Also, fire causes sudden variations in the carbon and energy balance
32 of ecosystems (Novara et al., 2013; Harris et al., 2016; Pausas & Millán, 2019) and in the soil microbial activity and functional
33 diversity of the microbiome (Velasco et al., 2009; Goberna et al., 2012).

34 At the onset of human civilisations, Mediterranean landscapes have been deeply modified by anthropogenic fires that were
35 used to expand the open-canopy space available for human activities and facilitate a wide array of foraging activities (Pausas
36 and Keeley, 2009). Throughout human history, demographic fluctuations, innovations and cultural exchanges have always
37 been accompanied by changes in land use and thus in fire regimes, amount and patchiness of fuel (Guyette et al., 2002; Driscoll
38 et al., 2021).

39 After the mid-20th century, land abandonment associated with an increase of woody cover and the build-up of fuels (Mantero
40 et al., 2020) chiefly contributed to the increased fire hazard in the Mediterranean Region (Le Houérou, 1993; Salis et al., 2022).
41 Despite the occurrence of some natural factors favouring fires, most of them are ignited by men through carelessness or
42 voluntary action. Being the vegetation burning strongly related to plant water content (Bond and Wilgen, 1996), fires happen
43 mostly during the warmest and driest months, i.e. during the Mediterranean summer (Bergmeier et al., 2021). Climate change
44 scenarios indicate rising temperatures and decreasing amounts of precipitation, resulting in longer summer aridity, soil water
45 shortages and increasing fire risk (Moriendo et al., 2006; Lozano et al., 2017; IPCC, 2021), despite lower productivity may
46 limit fuel availability (Baudena et al. 2020).

47 Nevertheless, typical Mediterranean shrublands are highly resilient to relatively frequent, high-intensity fires, but changes in
48 the fire regime may make these communities susceptible to compositional changes, potentially followed by alien plant
49 invasions (Keely and Brennan, 2012; Vallejo et al., 2012). The positive feedback between invasive species and fire can be a
50 major cause of unidirectional change in invaded ecosystems (Brooks et al., 2004), and invasive species able to sustain an
51 increased fire frequency and intensity may generate favourable conditions for their self-perpetuation (Pauchard et al., 2008).
52 Small islands are particularly vulnerable to biological invasions (Bellard et al., 2016), due to the combined effect of the reduced
53 species pool and the competitive traits of invasive species. This process has been reported for Mediterranean islands (Celesti-
54 Grapow et al., 2016; Fois et al., 2020), particularly in the case of volcanic islands with ongoing or recent volcanic activity
55 (Karadimou et al., 2015; Pasta et al., 2017; Chiarucci et al., 2021).

56 The island of Stromboli is the summit of the youngest and most active volcanic complex in the Aeolian Archipelago (NE-
57 Sicily); its subaerial activity began around 85 ka BP (Francalanci et al., 2013) and the emerged part consists of a single cone
58 rising up to 926 m above sea level. Stromboli has the lowest number of species, as expected by the within archipelago species-
59 area relationship among the seven largest islands of the Aeolian Archipelago, both for native and alien species (Chiarucci et
60 al., 2021). By far the most common invasive alien species in Stromboli is *Saccharum biflorum* Forssk. [= *S. spontaneum* L.
61 subsp. *aegyptiacum* (Willd.) Hack.; henceforth: *Saccharum*], a is a vigorously growing rhizomatous grass of Palaeotropical
62 origin (Amalra and Balasundaram, 2006) with culms 1.5-2.5 m and flowering stems up to 3 m high. Its rhizomes can be up to
63 6 m long, with nodes every 10-15 cm, from which the culms and fascicled roots branch off (Supplement 1, Fig. S1). This
64 species has a C₄ metabolism and thrives in sandy-silty, often alluvial soils (Pignatti et al., 2017-2019).

65 *Saccharum* was introduced in the 19th century as a windbreak. Gussone (1832) recorded its occurrence (despite wrongly
66 identifying it as *Saccharum ravennae* L.) on the islands of Stromboli, Panarea, Lipari and Vulcano, as “cultivated hedges in
67 vineyards”. *Saccharum* has then spread on former cultivations, abandoned terraced fields and wherever there was accumulation
68 of volcanic ash, as noticed by Ferro and Furnari (1968): “a large part of the north-eastern slope of the island, the very slope
69 that Lojacono (1878) travelled through ‘vineyards that produce beautiful wines’, is covered by dense, almost monophytic
70 *Saccharum* vegetation, from sea level up to the upper limit of the ancient crops (...). This slope could have been colonised in
71 a different way by native floristic elements, but it is difficult to make predictions on the final outcome of the competition,
72 given the compactness of the *Saccharum* rhizomatous apparatus”.

73 However, photos published by Ferro and Furnari (1968) give the impression that 50 years ago *Saccharum* was more widespread
74 than nowadays. Besides cultivation abandonment, the establishment of this plant is favoured by fire, as observed by Richter
75 (1984). Local elder people recall a major spread of *Saccharum* soon after the fire caused by paroxysmal activity in 1930 and
76 the subsequent abandonment of a large portion of the cultivated terraces along the eastern slopes of the island (Richter and
77 Lingenhöhl, 2002). In following years, the spread of this species has been somewhat reduced by the development of native
78 shrubland, which until recently was the most widespread vegetation type on the island. Another large fire event, ignited at the
79 Punta Labronzo landfill site in 1978, promoted the recovery of *Saccharum* all over the eastern slopes above Punta Labronzo.
80 On 25-26 May 2022, a large fire event burned much of the northern and eastern slopes of Stromboli, upstream of the villages
81 San Vincenzo and San Bartolo. This study uses remotely sensed data to analyse the post-fire damage on local vegetation

82 through the application of a spectrally sensitive index, i.e. the differential Normalised Burned Index (dNBR), which has been
83 used also to quantify the extent of the subsequent early-stage vegetation recovery, dominated by *Saccharum*, in order to
84 highlight the ecological behaviour of this invasive alien species and its fire-driven ability to colonise new spaces.

85 **Material & Methods**

86 *Study area.* The island of Stromboli, 12.6 km², represents the northeastern end of the Aeolian Archipelago, in southeastern
87 Tyrrhenian Sea, Mediterranean biogeographical region (Cervellini et al., 2020). The island has quite a regular slope averaging
88 28° and two large horseshoe-shaped flank collapses named “Sciara del Fuoco”, on the northwestern-, and “Rina Grande”, on
89 the southeastern flank.

90 Our study area covers an area of ca 3.4 km², between 50 m a.s.l. and 530 m a.s.l., on the northern and eastern sides of the
91 volcano and can be roughly divided in two sectors. The northern sector is bounded by the “Fili del Fuoco” ridge, overlooking
92 “Sciara del Fuoco”, to the west and by the Vallonazzo valley to the east; the eastern sector is bounded by the Vallonazzo valley
93 to the north-west and by the “Rina Grande” depression to the south-east (Fig. 1). Both sectors are characterised by medium to
94 gentle slopes, with 80% of the area sloping less than 30° (Fornaciai et al., 2010).

95 The climate of Stromboli is typically Mediterranean. At 4 m a.s.l. the average yearly temperature is 18.2 °C, with a mean
96 temperature of 12.3 °C in the coldest (January) and 26 °C in the warmest month (August). The annual rainfall averages 570
97 mm, while the relative humidity is 75.0% in winter and 60.8% in summer. Based on the WorldClim interpolated maps (Hijmans
98 et al., 2005) and on the Rivas-Martínez bioclimatic classification (2004), the study area is characterised by an upper thermo-
99 mediterranean thermotype and a dry to sub-humid ombrotype (Bazan et al., 2015).

100 The study area was dominated by a typical Mediterranean rockrose garrigue (*Cistus creticus* subsp. *eriocephalus*, *C.*
101 *monspeliensis*, *C. salvifolius*) with scattered patches of maquis with *Genista tyrrhena*, *Spartium junceum*, *Olea europaea*,
102 *Erica arborea* and *Pistacia lentiscus* (Richter, 1984; Cavallaro et al., 2009). The former cultivated land and the volcanic ash
103 deposits were extensively colonised by *Saccharum*, while small *Quercus ilex* stands were occasionally found along the
104 impluvium lines. Equally rare and scattered were the patches dominated by *Euphorbia dendroides*, limited to the rocky
105 outcrops, especially along the south-facing rim of Vallonazzo valley (Ferro and Furnari, 1968; Richter and Lingenhöhl, 2002).
106 The highest and southernmost end of the study area included part of the local population of *Cytisus aeolicus*, a narrow ranging
107 endemic broom growing only on the islands of Vulcano, Alicudi and Stromboli (Zaia et al., 2020).

108 On 25-26 May 2022, due to recklessness during the filming of a television drama, a fire broke out in the upper outskirts of the
109 village of San Vincenzo and, fuelled by a strong sirocco wind, burned the whole of our study area. While *Saccharum* stands
110 were entirely burned, a very few small patches of garrigue and *Quercus ilex* stands escaped from the fire.

112 *Satellite imagery processing.* To infer the extent of fire damage to the vegetation and the post-fire surface of the resprouted
113 *Saccharum* patches, we used optical satellite images acquired by the spaceborne Sentinel-2 sensor, a multispectral mission
114 launched in the frame of the European Space Agency (ESA) Copernicus program (Drusch, 2012).

115 Sentinel-2 measures globally the backscattered solar radiation from ground targets with a temporal resolution of around 5 days,
116 across 13 spectral bands with different ground sampling distance (GSD) varying from 10 to 60 metres. In this work, we
117 employed the four bands at 10 m GSD, namely in the visible range (blue, green, red) and near infrared (NIR). Additionally,
118 we relied on Band 12 in the short-wave infrared (SWIR) at 20 m GSD in order to detect burned areas. Additionally, spectral
119 bands 5, 6, 7, 8a, and 11, all at 20 m GSD, were used for the supervised classification of different vegetation types. All other
120 bands at 60 m GSD were not used in this analysis. The products used were at processing level 2A, which provides
121 radiometrically corrected, georeferenced, orthorectified, atmospherically corrected, and converted to bottom of atmosphere
122 reflectance data. The choice of using reflectance rather than radiance products is motivated by the following reasons: (1)

123 overall brightness differences in different images due to different acquisition conditions are reduced in the level 2A products,
124 (2) quantities estimated from single images through spectral indices result more meaningful when applied to data in reflectance.
125 The data selection and processing were carried out on Google Earth Engine (GEE) (Amani et al., 2020), which is at the same
126 time a multi-petabyte repository of geo-referenced and harmonised Earth Observation raster, vector, and tabular datasets,
127 which includes the whole Sentinel-2 archive.

128 To quantify the damage caused by the above mentioned fire event on the vegetation, different Sentinel-2 scenes acquired in a
129 relatively short time span were aggregated. An image composite of the island before the event was derived by considering 8
130 acquisition dates with cloud cover below 5% acquired before the fire event, from April 15 to May 22, 2022, and considering
131 the median reflectance for each image element. This allows removing abnormal values due to specific atmospheric conditions
132 inducing error in the reflectance estimation process, undetected clouds, and cloud shadows in the scene. The post-fire
133 reflectance was estimated by applying the same processing to 6 acquisition dates after the event, from May 26 to June 15,
134 2022. The two image composites are reported in Fig. 2. Therein, pre- and post-event true colour images obtained from Sentinel-
135 2 bands in the visible range (namely bands 4, 3, and 2) can be visually assessed, with damage caused by the fire in the
136 northeastern part of the island already evident in this band combination.

137 In order to estimate vegetation loss and total burned area, we derived the Normalised Burn Ratio (*NBR*), defined for a
138 multispectral image x as:

$$139 \quad NBR(x) = \frac{NIR - SWIR}{NIR + SWIR}$$

140 where *NIR* and *SWIR* indicate reflectance in the Near and Short-wave Infrared, represented for Sentinel-2 by the bands 8 and
141 12, respectively. The *NBR* is a commonly used index to detect burned area and burn severity (Key and Benson, 1996), and is
142 particularly sensitive to the changes in the amount of live green vegetation, moisture content, and some soil conditions which
143 may occur after fire (Lentile et al., 2006).

144 Change detection relying on spectral indices from multitemporal pre- and post-fire images can be used to estimate vegetation
145 loss or recovery. Relying on the availability of multitemporal images, we used the differenced *NBR* (*dNBR*) since it performs
146 well in capturing the spatial severity within fire perimeters (Picotte and Robertson, 2010; Soverel et al., 2010).

147 The *dNBR* related to pre- and post-event images, respectively x_{t_0} acquired at time t_0 and x_{t_1} acquired at time t_1 , is the delta
148 of the two measurements:

$$149 \quad dNBR(x_{t_0}, x_{t_1}) = NBR(x_{t_0}) - NBR(x_{t_1})$$

150 This quantity has been used to estimate both fire severity and vegetation recovery after the fire event: a negative *dNBR* is
151 correlated to recovery after fires, while a positive one indicates damages, with severity proportional to the *dNBR* value.

152 We first estimated the area affected by fire immediately after the event by computing the *dNBR* for the whole island. The
153 affected area was derived by applying the damage classes defined in (Key and Benson, 1996). In particular, the value of *dNBR*
154 in the middle of the range related to low-severity damage (0.1-0.27) and approximated to the second decimal digit, in the
155 specific 0.19, was selected and assessed using expert knowledge in order to exclude false positives from the estimation and
156 perform further analysis only on relevant image elements, considering damaged all image elements with *dNBR* above this
157 threshold (Fig. 2). This was necessary as using the value of 0.1 was raising false alarms, most notably within urban areas.

158 To check whether the severity of the damage was related to geomorphological features, rather than to different vegetation
159 units, the correlation between results of the *dNBR* and a digital elevation model (DEM), was evaluated. The Normalized
160 Difference Vegetation Index (*NDVI*; Gandhi et al., 2015) was also applied to estimate the loss in live green vegetation, and its
161 correlation with *dNBR* values was checked (Supplement 2).

162 Finally, to evaluate the quality of our results, we computed a new *dNBR* between the pre-event image and a mosaic of Sentinel-
163 2 acquisitions from the time range 15-17 August 2022. The burned area detected in such way was compared with very high-
164 resolution images acquired by a drone DJI Phantom 3 professional on 17 August 2022, i.e. around 3 months after the fire event
165 and 5 days after the first intense rainstorm. Drone images were merged and geo-referenced through the software Agisoft

166 Photoscan Professional (version 1.2.6). These images have 10 cm GSD and have been mosaicked over the north-eastern part
167 of the island, covering the inhabited area of San Bartolo and San Vincenzo. The drone images did not cover the higher
168 elevations of our study area, closer to the volcano's vents, nor the northernmost part, near Punta Labronzo (Fig. 4).
169

170 *Vegetation recovery assessment.* The mentioned image composite of Stromboli derived from 8 acquisitions from April-May
171 2022 was also used to map the structural types of the vegetation affected by the fire, through supervised classification based
172 on spectral information. Three vegetation classes have been defined: maquis, garrigue, and saccharum. The class "maquis"
173 groups tall woody vegetation patches, namely: (1) shrublands with *Genista tyrrhena*, *Spartium junceum*, *Erica arborea* and
174 *Pistacia lentiscus*, (2) abandoned olive groves invaded by *Cytisus infestus* and *C. laniger*, (3) *Quercus ilex* groves, (4)
175 *Euphorbia dendroides* shrublands, and (5) *Cytisus aeolicus* shrublands. The class "garrigue" refers to vegetation patches with
176 dwarf shrubs, subshrubs and bunchgrasses, including (1) dwarf shrublands dominated by *Cistus sp. pl.*, (2) herbaceous-
177 chamaephytic vegetation dominated by *Cymbopogon hirtus*, *Oloptum miliaceum*, *Centranthus ruber*, *Jacobaea maritima*
178 subsp. *bicolor* and *Scrophularia canina*, (3) small impluvia colonized *Rubus sp.* and *Pteridium aquilinum*. Finally, the
179 vegetation patches dominated by *Saccharum* were attributed to the "Saccharum" class, easily recognized by its typical
180 yellowish-green colour and remarkable structural homogeneity, due to one single species covering well over 80% of the soil.
181 These patches have two different textures: smoother where *Saccharum* has invaded abandoned vineyards, more granular where
182 *Saccharum* has invaded former fig tree plantations, as it happened in the upper part of our study area.

183 For each of the three classes described above, 10 patches of 50 pixels each were selected by experts to constitute the training
184 dataset and 150 random points equally split among the three classes constituted the validation dataset. The area where damage
185 occurred was fed to a Support Vector Machine (SVM) classifier (M.A. Hearst et al., 1998), as implemented in the *libsvm*
186 routine in GEE, using a linear kernel and setting the cost *C* to 1. The input parameters were all Sentinel-2 spectral bands having
187 a Ground Sampling Distance of 10 or 20 meters, namely bands 2 to 8, 8a, 11, and 12. The results of the classification algorithm
188 (Fig. 3) were evaluated through visual analysis by the experts and numerically validated using the validation dataset, yielding
189 an overall accuracy higher than 90%.

190 To check variations in the distribution of burn severity levels and to evaluate the short-term response after fire among different
191 vegetation types, the pixel values of *dNBR* pre-post were randomly sampled in 50 random points for each of the three
192 vegetation classes described above. Levene's test was used to assess the homogeneity of variance, followed by nonparametric
193 Kruskal-Wallis test, using Chi-Square distribution (right-tailed) and Dunn's post hoc comparison to reject the null hypothesis.
194 To evaluate the short-term vegetation response after fire, the composite images of Sentinel-2 acquisitions from the following
195 time ranges were analyzed: 15-17 August 2022; 14-26 September 2022; 22-28 October 2022; 10 May-15 June 2023.

196 On-site surveys were carried out on 15-19 September 2022, 7-9 March and 9-12 September 2023, in order to validate the
197 remotely sensed data and to sample vegetation plots in the burned area. The vegetation was sampled in 38 permanent plots,
198 10 m² each, randomly selected along a belt between 180 and 220 m elevation (Fig. 1). To optimize the sampling effort, the
199 location of the sampling sites deviated little from the paths that run along the volcano's flank above the villages of St. Vincent
200 and St. Bartolo. The only rules adopted were that the plots should have been at least 50 m apart, to avoid spatial autocorrelation,
201 and that each of the above-mentioned three vegetation classes should have been represented by at least 10 plots. Vegetation
202 data were collected using a modified Braun-Blanquet (1964) approach, by visually estimating the cover-abundance in
203 percentage values and by measuring the mean and maximum height (in cm) of each species.

204 In order to collect useful information to better understand the interaction between *Saccharum* and fire, a comparative evaluation
205 of stem density/m² in burned vs. unburned patches, was carried out in the field on 18 September 2002. Sampling plots 1 × 1
206 m were located every 100 m along two almost contiguous transects, 900 m long, ten inside the burned area, above the village
207 of San Vincenzo and 10 outside the burned area, in the bottom part of Rina Grande (Fig. 1). In each plot, the number of stems
208 of *Saccharum* was counted and the average and max. height were recorded. In the unburned patches, the relative percentage

209 of dry stems compared to green stems was also assessed, to showcase the ease of fire ignition due to the abundant presence of
210 dry biomass, consisting mainly of the flowering stems of *Saccharum* which, once faded, dry out completely but remain
211 standing, as they are supported by the green stems which have not yet flowered.
212

213 **Results**

214 The application of the *dNBR* yielded a severity map showing the difference between pre- and post-fire acquisitions. The burned
215 area was quantified in 337.83 ha, corresponding to 27.7% of the island surface (Fig. 2). Concerning the burn severity (Keeley
216 2009), 75.15 ha showed low, 218.37 ha intermediate and 44.31 ha high severity level. The Kruskal-Wallis H test indicated a
217 significant difference in the distribution of severity levels among vegetation classes, $\chi^2(2) = 8.56$, $p = .013$, having the burned
218 garrigue and maquis suffered higher severity damage than *Saccharum* (Fig. 3).

219 We found no correlation between the *dNBR* and neither the elevation nor the slope (therefore not reported here). *NDVI* values
220 were strongly correlated with *dNBR* values (Pearson correlation of 0.97, see Supplement 2). However, *NDVI* showed some
221 noise in the estimation of vegetation loss, and false positives scattered across the inhabited area. Therefore, these results are
222 not reported further in this paper, despite of *NDVI* having a true resolution of 10 m in Sentinel-2 products, while *NBR* employs
223 the SWIR band, which is originally at 20 m GSD and therefore interpolated.

224 Considering the limitations imposed on spatial resolution by the satellite-derived damage evaluation, the burned area detected
225 by *dNBR* from the mosaic of Sentinel-2 acquisitions in the time range 15-17 August 2022 matched well the burned area
226 observable in the drone image acquired on August 17th, with man-made structures and even single trees that were spared by
227 the fire correctly regarded as undamaged in the *dNBR* estimation (Fig. 4). At the same time, partially burned vegetated areas
228 were correctly included in *dNBR* results, because even if they did not burn completely a steep decrease in the red edge portion
229 of the spectrum around 700 nm revealed strong vegetative stress.

230 The *NDVI* calculated with a threshold of 0.08, therefore quantifying all pixels having at least 8% covered by photosynthetically
231 active vegetation, quantified the area of the island covered by vegetation before the fire as 678.73 ha. Considering the described
232 correlation between *dNBR* and *NDVI*, and the area affected by the fire as computed by *dNBR*, it can be concluded that roughly
233 half (49.8%) of the vegetated area of Stromboli has been burned during the fire event.

234 Figure 5 shows the vegetation recovery in the area affected by the fire. According to the thresholds suggested by Key and
235 Benson (1996) to categorise recovery levels from *dNBR* values, in the specific enhanced low and high regrowth for *dNBR*
236 values ranging from -100 to -250 and smaller than -250, respectively, one year after fire 53.25% of the burned area showed
237 high enhanced recovery, 30.84% low recovery, 15.9% no recovery. Among the three vegetation classes considered, 56.08%
238 of the pixels with high recovery levels were *Saccharum*, 38.2% garrigue and 5.7% maquis. Conversely, 10.46% of the areas
239 with no recovery were maquis, 65.48% garrigue and 23.856% *Saccharum*. Considering the distribution of recovery levels
240 across the first growing season after fire, *Saccharum* is clearly characterized by faster recovery with respect to the maquis and
241 the garrigue, particularly at the beginning of the first growing season after fire (September-October 2022).

242 Referring to the vegetation recovery estimated in October 2022, the Kruskal-Wallis H test indicated that there is a significant
243 difference among the vegetation classes, $\chi^2(2) = 8.41$, $p = .015$, with a mean rank score of 64.06 for *Saccharum*, 89 for garrigue,
244 and 73.44 for maquis. The Post-Hoc Dunn's test using a Bonferroni corrected alpha of 0.017 indicated significant differences
245 of *Saccharum* recovery towards both maquis and garrigue (Table 1).
246

247 **Table 1. Dunn's post hoc comparison for *dNBR*-estimated recovery of the considered vegetation classes in the burned**
248 **area on October 2022.**

Pair	Mean Rank difference	Z	SE	p-value	p-value/2
<i>Saccharum</i> -maquis	-24.94	2.8703	8.6891	0.004101	0.002051
<i>Saccharum</i> -garrigue	15.56	1.7908	8.6891	0.07333	0.03667
garrigue-maquis	-9.38	1.0795	8.6891	0.2804	0.1402

249

250

251

252

253

254

255

256

257

258

259

260

The results of the spectral evaluation of the vegetation recovery are confirmed by the on-site surveys. Table 2 shows the median values of percentage cover and height of resprouts and seedlings in the plots sampled on September 2022, March and September 2023. The distribution of the plots across the vegetation classes was the following: 10 *Saccharum*, 16 Garrigue, 12 Maquis. The Kruskal-Wallis H test indicated highly significant differences ($p < 0.001$) between the cover values and height of resprouts and cover of seedlings in the *Saccharum* plots compared to those ascribed to the other two vegetation classes. No significant difference was found in seedlings height or even in species composition across the vegetation classes (data not shown), which in all cases was largely dominated by annual plants such as *Brassica fruticulosa*, *Ornithopus compressus*, *Lupinus angustifolius*, *Trifolium stellatum* and by seedlings of *Cistus* sp.pl. (mainly *Cistus creticus*).

Table 2. Median values of cover (%) and height (cm) of resprouts and seedlings in the validation plots. Values in brackets indicate positive absolute deviations from the median values.

Date	Vegetation	Resprouts cover	Resprouts height	Seedlings cover	Seedlings height
15-19 Sept. 2022	<i>Saccharum</i>	85 (5)	150 (20)	5 (0)	9 (13)
	Garrigue	10 (15)	8 (17)	25 (25)	13 (21)
	Maquis	15 (15)	15 (12)	30 (30)	14 (16)
7-9 March 2023	<i>Saccharum</i>	90 (0)	160 (20)	10 (5)	43 (14)
	Garrigue	20 (10)	23 (24)	40 (20)	33 (22)
	Maquis	20 (15)	27 (38)	50 (25)	38 (25)
9-12 Sept. 2023	<i>Saccharum</i>	90 (0)	160 (20)	10 (10)	53 (19)
	Garrigue	25 (15)	20 (32)	55 (15)	47 (32)
	Maquis	25 (30)	36 (47)	50 (20)	55 (30)

261

262

263

264

265

The estimated vegetation composition in the study area shows that already in August resprouting *Saccharum* had invaded approximately 13% of areas previously occupied by other vegetation classes, especially along gullies. This latter percentage remained almost unchanged in the following months (Fig. 6). The fast recovery of the *Saccharum* patches, with their soft green colour standing out against the surrounding black, became evident as early as a few weeks after the fire (Supplement 1, Fig.

266 S3-5). Until first rains, which occurred on the night of 12 August 2022, *Saccharum* was the only green spot in the fire-affected
267 areas and the high-resolution drone images captured on 17 August 2022 clearly show all *Saccharum* patches in their recovery
268 phase (Fig. 4). In the Sentinel2 images of September-October 2022, previous damage from the fire event appears mitigated.
269 More in detail, a total of 110 ha of the previously burned area (roughly one third) exhibits a *dNBR* value below -0.1, which
270 represents a strong indicator of vegetation recovery. This was mostly due to *Saccharum*, demonstrating that this species can
271 exert unchallenged dominance in the early stages of the post-fire dynamics (succession), reaching vegetative stem densities
272 only slightly lower than those of the unburned stands in a short time (Fig. 7).

273 Discussion

274 Our study confirms that fire severity can be mapped with high accuracy using indices derived from Sentinel 2 imagery with
275 supervised vegetation classification based on spectral information (Gibson et al. 2020). Fire is a major driving force for
276 Mediterranean insular ecosystem dynamics since the emergence of the Mediterranean climate (Médail, 2021), particularly in
277 volcanic island ecosystems (Irl et al., 2014). This paper provides the first report of how a single fire event significantly affected
278 Stromboli Island, burning 50% of the vegetated island surface. This clearly influenced the island biota, particularly the native
279 vegetation, which is rich in species of relevant biogeographic interest, such as *Centaurea aeolica*, *Genista tyrrhena*, *Dianthus*
280 *rupicola* subsp. *aeolicus*, *Jacobaea maritima* subsp. *bicolor* (Pasta et al., submitted). In addition, the highest and southernmost
281 end of the study area included part of the *Cytisus aeolicus* population, one of the rarest and most emblematic endemic plant
282 species of the Aeolian Archipelago (Zaia et al., 2020).

283 Although we applied a permissive threshold (8%) in the NDVI for our quantitative analysis, our conclusion that the fire
284 occurred on 25-26 May 2022 burned roughly half of Stromboli's vegetated area appears reasonably accurate, when considering
285 all the available data we used for validation. Our study confirms that burn severity levels, estimated by *dNBR*, is higher in
286 woody vegetation (Koutsias & Karteris, 2002), presumably due to the larger above-ground biomass and dead organic matter
287 stock in the case of maquis (Rossetti et al. 2022) and to the high flammability of Mediterranean dwarf shrubs in the case of
288 garrigue (Dimitrakopoulos, 2001). Despite the garrigue being mostly formed by pyrophytes, obligate seeders, and among the
289 first shrubs to emerge after fire (Palá-Paúl, 2005; Athanasiou et al., 2023), our study demonstrated that *Saccharum* exhibits
290 even greater resilience compared to garrigue in the earliest stages after fire, with a clear risk of altering the recovery patterns
291 of native vegetation, that especially on volcanic islands are characterized by high abundance of nitrogen fixers and annual
292 species (Weiser et al., 2021).

293 The positive interaction between *Saccharum* and fire was already noticed in Stromboli by Richter (1984) and Richter and
294 Lingenhöhl (2002). Fire spreads very easily across *Saccharum* vegetation, due to the abundant presence of standing dry
295 biomass (Supplement 1, Fig. S2, S4, S6). This result agrees with many recent studies focused on the role of fire as promoter
296 of C₄ grasses (Scheiter et al., 2012; Hoetzel et al., 2013; Ripley et al., 2015). Although the native rockrose garrigue vegetation
297 is also adapted to - and favoured by - periodical fires (Pausas, 1999), its survival derives from the ability of *Cistus* to develop
298 a long-lasting soil seed bank (Soy and Sonie, 1992; Scuderi et al., 2010). Too frequent fire events and runoff caused by heavy
299 rainfall on sandy and incoherent soils may cause a critical depletion of soil seed bank and favour sprouters against obligate
300 seeders. On this purpose, we must point out that the autochthonous sprouters (such as *Erica arborea*, *Pistacia lentiscus*, *Olea*
301 *europaea*) have slower growth rate than *Saccharum* and need longer time to become established.

302 After the fire, our study area was exposed to full solar radiation; dark sandy surfaces were subject to extreme microclimatic
303 (surface temperatures up to 80 °C; see Richter, 1984) and extremely dry conditions. These were not favourable for the
304 germination of the soil seed bank, whilst sprouters faced almost no competition until first rains, which occurred on 12 August
305 2022. The first and most important beneficiary of these contrasting conditions was *Saccharum*, which over time was able to
306 colonise large surfaces of tephra in the northern and eastern parts of the island, likely due to a positive interaction between
307 land abandonment, repeated fires and volcanic ash deposition. *Saccharum* is extremely competitive thanks to a variety of

308 functional strategies (e.g. C4 photosynthetic pathway, large resource allocation belowground, into clonal and bud-bearing
309 rhizomes which can boost a quick resprouting and local spread/space occupancy/resource uptake) under current and probably
310 also under predicted conditions (likely more disturbed) which could affect and define different ecosystems on Stromboli.
311 According to Lojacono (1878), *Saccharum* was planted along the vineyards to shelter them from the northerly winds (Fig. 8).
312 This condition lasted until the eruption of 11 September 1930, so far considered the most violent and destructive event in the
313 historical records of Stromboli's activity (Rittmann, 1931). Facilitated by the winter rains and by a rapid expansion via
314 rhizomes, *Saccharum* first benefited from the emigration of most inhabitants and subsequent abandonment of terraced fields,
315 which in a very short time lapse were almost completely sealed off by a dense monospecific bed, which made it difficult for
316 other species to establish themselves (Ferro and Furnari, 1968; Richter, 1984). Since then, competition for space between local
317 native vegetation and *Saccharum* beds has been regulated mainly by the periodical occurrence of fires. Further studies are
318 needed to understand the duration of the *Saccharum* expansion phases. Our preliminary results suggest that the expansion of
319 *Saccharum* is surprisingly fast, but the decline may also be relatively rapid. There is no data on the longevity of *Saccharum*
320 rhizomes and related senescence processes, nor on the effects of volcanic ash deposition on rhizome burial. However, there
321 are reasonable indications that, if the vegetation is not too frequently affected by fire, *Saccharum* could be gradually replaced
322 by native vegetation within a few decades, as captured in the maps published as "Fig. 4" by Richter and Lingenhöhl (2002).
323 On 12 August 2022, a severe thunderstorm triggered disastrous erosion processes over the entire area affected by the fire on
324 May 25-26. Large quantities of mud, stones and volcanic ashes flooded the streets of the villages San Bartolo and San Vincenzo
325 (Supplement 1, Fig. S7). In the burned area, the traces of runoff and surface rill erosion were still very evident during our
326 inspections on 18-19 September 2022. However, just as evident was the ambivalent role of *Saccharum*, which, while on the
327 one hand clearly prevails on native species, on the other hand, thanks to its dense mat of rhizomes, proves to be much more
328 efficient than the burned native vegetation in counteracting hydrogeological instability. The latter is a very relevant aspect in
329 a volcanic island, whose soils are largely made up of loose tephra ashes.

330 Over time, *Saccharum* beds have become an important secondary habitat for many animal species. In fact, they represent the
331 main breeding site for at least 70% of breeding bird species on Stromboli (Massa et al., 2015) and host conspicuous populations
332 of almost all terrestrial vertebrates occurring on the island (especially *Tarentola mauritanica*, *Podarcis siculus* and *Hierophis*
333 *viridiflavus*). Some of the invertebrates that occurs in the *Saccharum* beds are of considerable biogeographic interest, such as
334 *Caulostrophus zancleanus*, a regional endemic (Lo Cascio et al., 2022), and the recently described *Catomus aeolicus*, endemic
335 of the northeastern sector of the Aeolian archipelago (Ponel et al., 2020). Although not specialised on *Saccharum*, the
336 rhizophagous larvae of the melolonthid *Anoxia orientalis*, a species considered rare at national scale in Italy, feed on its
337 rhizomes. Surprisingly enough, *S. biflorum* does not seem to be an attractive fodder for the mammals introduced in historical
338 (*Oryctolagus cuniculus*) or more recent (*Capra hircus*) times, nor significant infestations of phytophagous insects have ever
339 been observed. Thus, herbivory does not seem to be a limiting factor to the expansion of *Saccharum* on Stromboli.

340 **Conclusions**

341 Remotely sensed data provide fast, accurate and reliable information for post-fire damage analysis, being spectrally sensitive
342 to vegetation features and structure. Multi-temporal data acquisition allows observations on early-stage vegetation dynamics
343 which, in our case, point out the outstanding pioneer role played by *Saccharum biflorum*, showcasing its ability to colonize
344 and dominate large areas, potentially altering the recovery patterns of native vegetation. On the other hand, *Saccharum* proves
345 to be efficient in stabilizing the soil, especially in a volcanic island with loose tephra ashes, thus mitigating the erosion
346 processes. Our findings underscore the complex interplay between fire, vegetation dynamics, and ecosystem recovery on
347 Stromboli, emphasizing the need for further research to better understand the long-term dynamics of *Saccharum* expansion
348 and its interactions with native biota.

349

350 *Author contribution.* RG and DC developed the research idea, DC processed satellite and drone imagery, RG and RZ conducted
351 the field work, RG led the writing process, all authors discussed the results and contributed to the manuscript.

352

353 *Acknowledgements.* We would like to thank Giuseppe De Rosa, who brought DC and RG together, and Antonio Zimbone for
354 driving the drone flight and taking the pictures used to check the quality of the information derived from dNBR analysis. Three
355 anonymous reviewers and Gianluigi Ottaviani are gratefully acknowledges for their suggestions on an earlier version of the
356 manuscript.

357

358 *Competing interests.* The contact authors declared that neither they nor their co-authors have any competing interests.

359 **References**

360 Amalraj, V. A., and Balasundaram, N.: On the taxonomy of the members of ‘*Saccharum* complex’. *Genetic Resources and*
361 *Crop Evolution*, 53, 35–41, <https://doi.org/10.1007/s10722-004-0581-1>, 2006.

362 Amani, M., Ghorbanian, A., Ahmadi, S. A., Kakooei, M., Moghimi, A., Mirmazloumi, S. M., Moghaddam, S. A. H., Mahdavi,
363 S., Ghahremanloo, M., Parsian, S., Wu, Q., and Brisco, B.: Google earth engine cloud computing platform for remote sensing
364 big data applications: A comprehensive review. *IEEE Journal of Selected Topics in Applied Earth Observations and Remote*
365 *Sensing*, 13, 5326–5350, <https://doi.org/10.1109/JSTARS.2020.3021052>, 2020.

366 Athanasiou, M., Martinis, A., Korakaki, E., and Avramidou, E. V.: . Development of a Fuel Model for *Cistus* spp. and Testing
367 Its Fire Behavior Prediction Performance. *Fire* 2023, 6, 247, <https://doi.org/10.3390/fire6070247>, 2023.

368 Baudena, M., Santana, V.M., Baeza, M.J., Bautista, S., Eppinga, M.B., Hemerik, L., Garcia Mayor, A., Rodriguez, F.,
369 Valdecantos, A., Vallejo, V.R., Vasques, A., and Rietkerk, M.: Increased aridity drives post-fire recovery of Mediterranean
370 forests towards open shrublands. *New Phytologist*, 225(4), 1500-1515, <https://doi.org/10.1111/nph.16252>, 2020.

371 Bazan, G., Marino, P., Guarino, R., Domina, G., and Schicchi, R.: Bioclimatology and vegetation series in Sicily: A
372 geostatistical approach, *Annales Botanici Fennici*, 52, 1–18, <https://doi.org/10.5735/085.052.0202>, 2015.

373 Bergmeier, E., Capelo, J., Di Pietro, R., Guarino, R., Kavgacı, A., Loidi, J., Tsiripidis, J., and Xystrakis, F.: ‘Back to the
374 Future’—Oak wood-pasture for wildfire prevention in the Mediterranean, *Plant Sociology*, 58, 41–48,
375 <https://doi.org/10.3897/pls2021582/04>, 2021.

376 Bellard, C., Cassey, P., and Blackburn, T. M.: Alien species as a driver of recent extinctions, *Biology Letters* 12, 20150623,
377 <https://doi.org/10.1098/rsbl.2015.0623>, 2016.

378 Bond, W. J., and Wilgen, B. W.: Why and how do ecosystems burn?, *Fire and plants: Population and Community Biology*
379 *Series 14*: 16–33. Springer, Dordrecht, 1996.

380 Brooks, M.L., D’Antonio, C.M., Richardson, D.M., Di Tomaso, J.M., Grace, J.B., Hobbs, R.J., Keeley, J.E., Pellant, M., Pyke,
381 D.: Effects of invasive alien plants on fire regimes. *Bioscience*, 54, 677–688, [https://doi.org/10.1641/0006-3568\(2004\)054\[0677:EOIAP0\]2.0.CO;2](https://doi.org/10.1641/0006-3568(2004)054[0677:EOIAP0]2.0.CO;2), 2004.

383 Canelles, Q., Aquilué, N., Duane, A., and Brotons, L.: From stand to landscape: modelling post-fire regeneration and species
384 growth, *Ecological Modelling*, 404, 103–111, <https://doi.org/10.1016/j.ecolmodel.2019.05.001>, 2019.

385 Cavallaro, F., Morabito, M., Navarra, E., Pasta, S., Lo Cascio, P., Campanella, P., Cavallaro, M., Cavallaro, A., Merenda, A.,
386 Di Procolo, G., Rühl, J. and Ioppolo, G.: Piano di Gestione dei Siti Natura 2000 delle Isole Eolie. Regione Siciliana,
387 Assessorato Territorio e Ambiente, 2009.

388 Celesti-Grapow, L., Bassi, L., Brundu, G., Camarda, I., Carli, E., D’Auria, G., Del Guacchio, E., Domina, G. Ferretti, G.,
389 Foggi, B., Lazzaro, L., Mazzola, P., Peccenini, S., Pretto, F., Stinca, A., and Blasi, C.: Plant invasions on small Mediterranean
390 islands: An overview, *Plant Biosystems*, 150(5), 1119–1133, <https://doi.org/10.1080/11263504.2016.1218974>, 2016.

391 Cervellini, M., Zannini, P., Di Musciano, M., Fattorini, S., Jiménez-Alfaro, B., Rocchini, D., Field, R., Vetaas O.R., Irl, S.D.H.,
392 Beierkuhnlein, C., Hoffmann, S., Fischer, J.-C., Casella, L., Angelini, P., Genovesi, P., Nascimbene, J. and Chiarucci, A.: A
393 grid-based map for the Biogeographical Regions of Europe. *Biodiversity Data Journal*, 8, e53720,
394 <https://doi.org/10.3897/BDJ.8.e53720>, 2020.

395 Chiarucci, A., Guarino, R., Pasta, S., La Rosa, A., Lo Cascio, P., Médail, F., Pavon, D., Fernández-Palacios, J. M., and Zannini,
396 P.: Species-area relationship and small-island effect of vascular plant diversity in a young volcanic archipelago, *Journal of*
397 *Biogeography*, 48(11), 2919–2931, <https://doi.org/10.1111/jbi.14253>, 2021.

398 Dimitrakopoulos, A.P.: A statistical classification of Mediterranean species based on their flammability components.
399 *International Journal of Wildland Fire*, 10, 113–118, <https://doi.org/10.1071/WF01004>, 2001.

400 Driscoll, D. A., Armenteras, D., Bennett, A. F., Brotons, L., Clarke, M. F., Doherty, T.S., Haslem, A., Kelly, L.T., Sato, C.F.,
401 Sitters, H., Aquilué, N., Bell, K., Chadid, M., Duane, A., Meza-Elizalde, M.C., Giljohann, K.M., González, T.M., Jambhekar,
402 R., Lazzari, J., Morán-Ordóñez, A. and Wevill, T.: How fire interacts with habitat loss and fragmentation, *Biological*
403 *Reviews*, 96(3), 976–998, <https://doi.org/10.1111/brv.12687>, 2021.

404 Drusch, M., Del Bello, U., Carlier, S., Colin, O., Fernandez, V., Gascon, F., Hoersch, B., Isola, C., Laberinti, P., Martimort,
405 P., Meygret, A., Spoto, F., Sy, O., Marchese, F., and Bargellini, P. : Sentinel-2: ESA's optical high-resolution mission for
406 GMES operational services, *Remote Sensing of Environment*, 120, 25–36, <https://doi.org/10.1016/j.rse.2011.11.026>, 2012.

407 Ferro, G. and Furnari, F.: Flora e vegetazione di Stromboli (Isole Eolie), *Archivio Botanico e Biografico Italiano*, 44(1–2),
408 21–45, 1968.

409 Fois, M., Podda, L., Médail, F., and Bacchetta, G.: Endemic and alien vascular plant diversity in the small Mediterranean
410 islands of Sardinia: Drivers and implications for their conservation, *Biological Conservation*, 244, 108519,
411 <https://doi.org/10.1016/j.biocon.2020.108519>, 2020.

412 Fornaciai, A., Bisson, M., Landi, P., Mazzarini, F., and Pareschi, M. T.: A LiDAR survey of Stromboli volcano (Italy): Digital
413 elevation model-based geomorphology and intensity analysis, *International Journal of Remote Sensing*, 31(12), 3177–3194,
414 <https://doi.org/10.1080/01431160903154416>, 2010.

415 Gibson, R., Danaher, T., Hehir, W., and Collins, L.: A remote sensing approach to mapping fire severity in south-eastern
416 Australia using sentinel 2 and random forest. *Remote Sensing of Environment*, 240, 111702,
417 <https://doi.org/10.1016/j.rse.2020.111702>, 2020.

418 Goberna, M., García, C., Insam, H., Hernández, M. T., and Verdú, M.: Burning fire-prone Mediterranean shrublands:
419 immediate changes in soil microbial community structure and ecosystem functions, *Microbial Ecology*, 64(1), 242–255,
420 <https://doi.org/10.1007/s00248-011-9995-4>, 2012.

421 Gussone, G.: *Supplementum ad Florae Siculae Prodrumum*, Edit. Tramater, Neapoli, 314 pp., 1832.

422 Gandhi, M., Parthiban, S., Thummalu, N. and Christy, A.: NDVI: Vegetation change detection using remote sensing and GIS
423 - A case study of Vellore District, *Procedia Computing Science* 57, 1199–1210, <https://doi.org/10.1016/j.procs.2015.07.415>,
424 2015.

425 Guyette, R. P., Muzika, R .M. and Dey, D. C.: Dynamics of an anthropogenic fire regime, *Ecosystems* 5(5), 472–486,
426 <https://doi.org/10.1007/s10021-002-0115-7>, 2002.

427 Harris, R. M., Remenyi, T. A., Williamson, G. J., Bindoff, N. L., and Bowman, D. M.: Climate–vegetation–fire interactions
428 and feedbacks: trivial detail or major barrier to projecting the future of the Earth system?. *Wiley Interdisciplinary Reviews:*
429 *Climate Change*, 7(6), 910–931, <https://doi.org/10.1002/wcc.428>, 2016.

430 Hijmans, R. J., Cameron, S. E., Parra, J. L., Jone, P. G. and Jarvis, A.: Very high resolution interpolated climate surfaces for
431 global land areas, *International Journal of Climatology* 25, 1965–1978, <https://doi.org/10.1002/joc.1276>, 2005.

432 Hoetzel, S., Dupont, L., Schefuß, E., Rommerskirchen, F., and Wefer, S.: The role of fire in Miocene to Pliocene C4 grassland
433 and ecosystem evolution, *Nature Geosciences*, 6, 1027–1030, <https://doi.org/10.1038/ngeo1984>, 2013.

434 Irl, S. D. H., Steinbauer, M. J., Messinger, J., Blume-Werry, G., Palomares-Martínez, Á., Beierkuhnlein, C., and Jentsch, A.:
435 Burned and devoured - Introduced herbivores, fire, and the endemic flora of the high-elevation ecosystem on La Palma, Canary
436 Islands, *Arctic, Antarctic, and Alpine Research*, 46(4), 859–869, <https://doi.org/10.1657/1938-4246-46.4.859>, 2014.

437 IPCC: Sixth Assessment Report. AR6 Climate Change 2021: The physical science basis.
438 <https://www.ipcc.ch/report/ar6/wg1/#Regional> [Accessed 28 November 2022].

439 Jouffroy-Bapicot, I., Pedrotta, T., Debret, M., Field, S., Sulpizio, R., Zanchetta, G., Sabatier, P., Roberts, N., Tinner, W.,
440 Walsh, K., and Vanni re, B.: Olive groves around the lake. A ten-thousand-year history of a Cretan landscape (Greece) reveals
441 the dominant role of humans in making this Mediterranean ecosystem, *Quaternary Science Reviews*, 267, 107072,
442 <https://doi.org/10.1016/j.quascirev.2021.107072>, 2021.

443 Karadimou, E., Tsiripidis, I., Kallimanis, A. S., Raus, T., and Dimopoulos, P.: Functional diversity reveals complex assembly
444 processes on sea-born volcanic islands, *Journal of Vegetation Science*, 26, 501–512, <https://doi.org/10.1111/jvs.12255>, 2015.

445 Keeley, J. E.: Fire intensity, fire severity and burn severity: a brief review and suggested usage. *International Journal of*
446 *Wildland Fire*, 18(1), 116-126, <https://doi.org/10.1071/WF07049>, 2009.

447 Keeley, J. E., and Brennan, T. J.: Fire-driven alien invasion in a fire-adapted ecosystem. *Oecologia*, 169(4), 1043–1052,
448 <https://doi.org/10.1007/s00442-012-2253-8>, 2012.

449 Key, C. H., and Benson N. C.: Landscape assessment (LA) sampling and analysis methods. USDA Forest Service, Rocky
450 Mountain Research Station, General Technical Report RMRS-GTR-164-CD, 2006.

451 Koutsias, N., and Karteris, M.: Classification analyses of vegetation for delineating forest fire fuel complexes in a
452 Mediterranean test site using satellite remote sensing and GIS. *International Journal of Remote Sensing*, 24, 3093–3104,
453 <https://doi.org/10.1080/0143116021000021152>, 2002.

454 Le Hou rou, H. N.: Land degradation in Mediterranean Europe: can agroforestry be a part of the solution? A prospective
455 review, *Agroforestry Systems* 21, 43–61, <https://doi.org/10.1007/BF00704925>, 1993.

456 Lentile, L. B., Holden, Z. A., Smith, A. M. S., Falkowski, M. J., Hudak, A. T., Morgan, P., Lewis, S. A., Gessler, P. E., and
457 Benson, N. C.: Remote sensing techniques to assess active fire characteristics and post-fire effects. *International Journal of*
458 *Wildland Fire*, 15, 319–345, <https://doi.org/10.1071/WF05097>, 2006.

459 Lo Cascio, P., Ponel, P. and Altadonna, G.: Diversity and distribution of beetles in a Mediterranean volcanic archipelago: an
460 updated checklist of the Coleoptera on the Aeolian Islands (Sicily, Italy). *Biodiversity Journal*, 13(3), 531–
461 585, <https://doi.org/10.31396/Biodiv.Jour.2022.13.3.531.585>, 2022.

462 Lojacono, M.: *Le Isole Eolie e la loro vegetazione, con enumerazione delle piante spontanee vascolari*. Palermo, Lorusnaider,
463 147 pp., 1878.

464 Lozano, O. M., Salis, M., Ager, A. A., Arca, B., Alcasena, F. J., Monteiro, A. T., Finney, M. A., Del Giudice, L., Scoccimarro,
465 E., and Spano, D.: Assessing climate change impacts on wild fire exposure in Mediterranean areas, *Risk Analysis*, 37, 1898–
466 1916, <https://doi.org/10.1111/risa.12739>, 2017.

467 Mantero, G., Morresi, D., Marzano, R., Motta, R., Mladenoff, D. J., and Garbarino, M.: The influence of land abandonment
468 on forest disturbance regimes: a global review, *Landscape Ecology* 35, 2723–2744, <https://doi.org/10.1007/s10980-020-01147-w>, 2020.

470 Massa, B., Lo Cascio, P., Ientile, R., Canale, E., and La Mantia, T.: Gli uccelli delle isole circumsiciliane, *Naturalista siciliano*,
471 39(2), 105–373, 2015.

472 M dail, F.: Plant Biogeography and Vegetation Patterns of the Mediterranean Islands, *The Botanical Review*, 88, 63–129,
473 <https://doi.org/10.1007/s12229-021-09245-3>, 2021.

474 Moriondo, M., Good, P., Durao, R., Bindi, M., Giannokopoulos, C., and Core-Real, J.: Potential impact of climate change on
475 fire risk in the Mediterranean area, *Climate Research*, 31, 85–95, <https://doi:10.3354/cr031085>, 2006.

476 Novara, A., Gristina, L., Rühl, J., Pasta, S., D'Angelo, G., La Mantia, T., and Pereira, P.: Grassland fire effect on soil organic
477 carbon reservoirs in semiarid environments, *Solid Earth*, 4(1-5), 1–13, <https://doi.org/10.5194/se-4-1-2013>, 2013.

478 Palá-Paúl, J., Velasco-Negueruela, A., Pérez-Alonso, M.J., and Sanz, J.: Seasonal variation in chemical composition of *Cistus*
479 *albidus* L. from Spain. *Journal of Essential Oil Research*, 17, 19–22, <https://doi.org/10.1080/10412905.2005.9698818>, 2005.

480 Pasta, S., Ardenghi, N. M. G., Badalamenti, E., La Mantia, T., Livreri Console, S. & Parolo, G.: The alien vascular flora of
481 Linosa (Pelagie Islands, Strait of Sicily): update and management proposals, *Willdenowia*, 47(2), 135–144,
482 <https://doi.org/10.3372/wi.47.47205>, 2017

483 Pasta, S., Guarino, R., La Rosa, A., Lo Cascio, P., Chiarucci, A., Médail, F., Pavon, D., Zannini, P., and Fernández-Palacios,
484 J.M., *Tentamen Florae Aeolicae*: comprehensive checklist and biogeographic analysis of the vascular flora of the Aeolian
485 Archipelago (Sicily, Italy), *Mediterranean Botany*, submitted.

486 Pauchard, A., García, R. A., Pena, E., González, C., Cavieres, L. A., and Bustamante, R. O.: Positive feedbacks between plant
487 invasions and fire regimes: *Teline monspessulana* (L.) K. Koch (Fabaceae) in central Chile, *Biological Invasions*, 10(4), 547–
488 553, <https://doi.org/10.1007/s10530-007-9151-8>, 2008.

489 Pausas, J. G.: Response of plant functional types to changes in the fire regime in Mediterranean ecosystems: a simulation
490 approach, *Journal of Vegetation Science*, 10(5), 717–722, <https://doi.org/10.2307/3237086>, 1999.

491 Pausas, J. G.: Simulating Mediterranean landscape pattern and vegetation dynamics under different fire regimes, *Plant*
492 *Ecology*, 187(2), 249–259, <https://doi.org/10.1007/s11258-006-9138-z>, 2006.

493 Pausas J. G. and Keeley, J. E.: A burning story: the role of fire in the history of life, *BioScience* 59(7), 593–601,
494 doi:10.1525/bio.2009.59.7.10, 2009.

495 Pausas, J. G., and Millán, M. M.: Greening and browning in a climate change hotspot: the Mediterranean
496 Basin, *BioScience*, 69(2), 143–151, <https://doi.org/10.1093/biosci/biy157>, 2019.

497 Picotte, J. J., and Robertson, K. M.: Accuracy of remote sensing wildland fire-burned area in southeastern US Coastal plain
498 habitats, *Tall Timbers Fire Ecol. Proc.*, 24, 86–93, 2010.

499 Pignatti, S., Guarino, R., and La Rosa, M.: *Flora d'Italia*, 4 vols. Edagricole, Edizioni Agricole di New Business Media,
500 Bologna.

501 Ponel, P., Lo Cascio, P., and Soldati, F.: A new species of *Catomus* Allard, 1876 (Coleoptera: Tenebrionidae: Helopini) from
502 the Aeolian Archipelago (Sicily, Italy), *Zootaxa*, 4743(2), 295–300, <https://doi.org/10.11646/zootaxa.4743.2.14>, 2020

503 Richter, M.: Vegetationsdynamik auf Stromboli, *Aachener Geographische Arbeiten*, 16, 41–110, 1984.

504 Richter, M., and Lingenhöhl, D.: Landschaftsentwicklung auf den Äolischen Inseln. Betrachtung in verschiedenen Zeitskalen,
505 *Geographische Rundschau*, 54(4), 20–26, 2002.

506 Ripley, B. S., Visser, V., Christin, P.-A., Archibald, S., Martin, T., and Osborne, C.: Fire ecology of C3 and C4 grasses
507 depends on evolutionary history and frequency of burning but not photosynthetic type, *Ecology*, 96(10), 2679–2691,
508 <https://doi.org/10.1890/14-1495.1>, 2015

509 Rittmann, M.: Der Ausbruch des Stromboli am 11. September 1930. *Zeitschrift für Vulkanologie*, 14, 47-77, 1931.

510 Rivas-Martínez, S. Clasificación Bioclimática de la Tierra, 2004,
511 https://webs.ucm.es/info/cif/book/bioc/global_bioclimatics_2.htm. [Accessed 28 November 2022]

512 Rossetti, I., Cogoni, D., Calderisi, G., and Fenu, G.: Short-Term Effects and Vegetation Response after a Megafire in a
513 Mediterranean Area. *Land*, 11(12), 2328, <https://doi.org/10.3390/land11122328>, 2022.

514 Roy, J., and Sonie, L.: Germination and population dynamics of *Cistus* species in relation to fire, *Journal of Applied Ecology*,
515 29(3), 647–655, <https://doi.org/10.2307/2404472>, 1992.

516 Salis, M., Del Giudice, L., Jahdi, R., Alcasena-Urdiroz, F., Scarpa, C., Pellizzaro, G., Bacciu, V., Schirru, M., Ventura, A.,
517 Casula, M., Pedes, F., Canu, A., Duce, P., and Arca, B.: Spatial patterns and intensity of land abandonment drive wildfire
518 hazard and likelihood in Mediterranean agropastoral areas, *Land*, 11(11), 1942, <https://doi.org/10.3390/land11111942>, 2022.

519 Scheiter, S., Higgins, S. I., Osborne, C. P., Bradshaw, C., Lunt, D., Ripley, B. S., Taylor, L. L., and Beerling, D. J.: Fire and
520 fire-adapted vegetation promoted C4 expansion in the late Miocene, *New Phytologist*, 195(3), 653–666,
521 <https://doi.org/10.1111/j.1469-8137.2012.04202.x>, 2012.

522 Scuderi, D., Di Gregorio, R., Toscano, S., Cassaniti, C., and Romano, D.: Germination behaviour of four mediterranean *Cistus*
523 *L.* species in relation to high temperature, *Ecological Questions*, 12, 171–180, <https://doi.org/10.12775/v10090-010-0011-2>,
524 2010.

525 Soverel, N.O., Perrakis, D. D. B., and Coops, N. C.: Estimating burn severity from Landsat d NBR and Rd NBR indices across
526 western Canada, *Remote Sensing of Environment*, 114, 1896–1909, <https://doi.org/10.1016/j.rse.2010.03.013>, 2010.

527 Trabaud, L.: Postfire plant community dynamics in the Mediterranean Basin, in: *The Role of Fire in Mediterranean-Type*
528 *Ecosystems*, edited by Moreno, J.M. and Oechel, W.C., Springer, New York, NY, 1–15, [https://doi.org/10.1007/978-1-4613-](https://doi.org/10.1007/978-1-4613-8395-6_1)
529 [8395-6_1](https://doi.org/10.1007/978-1-4613-8395-6_1), 1994.

530 Velasco, A. G. V., Probanza, A., Mañero, F. G., Treviño, A. C., Moreno, J. M., and Garcia, J. L.: Effect of fire and retardant
531 on soil microbial activity and functional diversity in a Mediterranean pasture, *Geoderma*, 153(1-2), 186–193,
532 <https://doi.org/10.1016/j.geoderma.2009.08.005>, 2009.

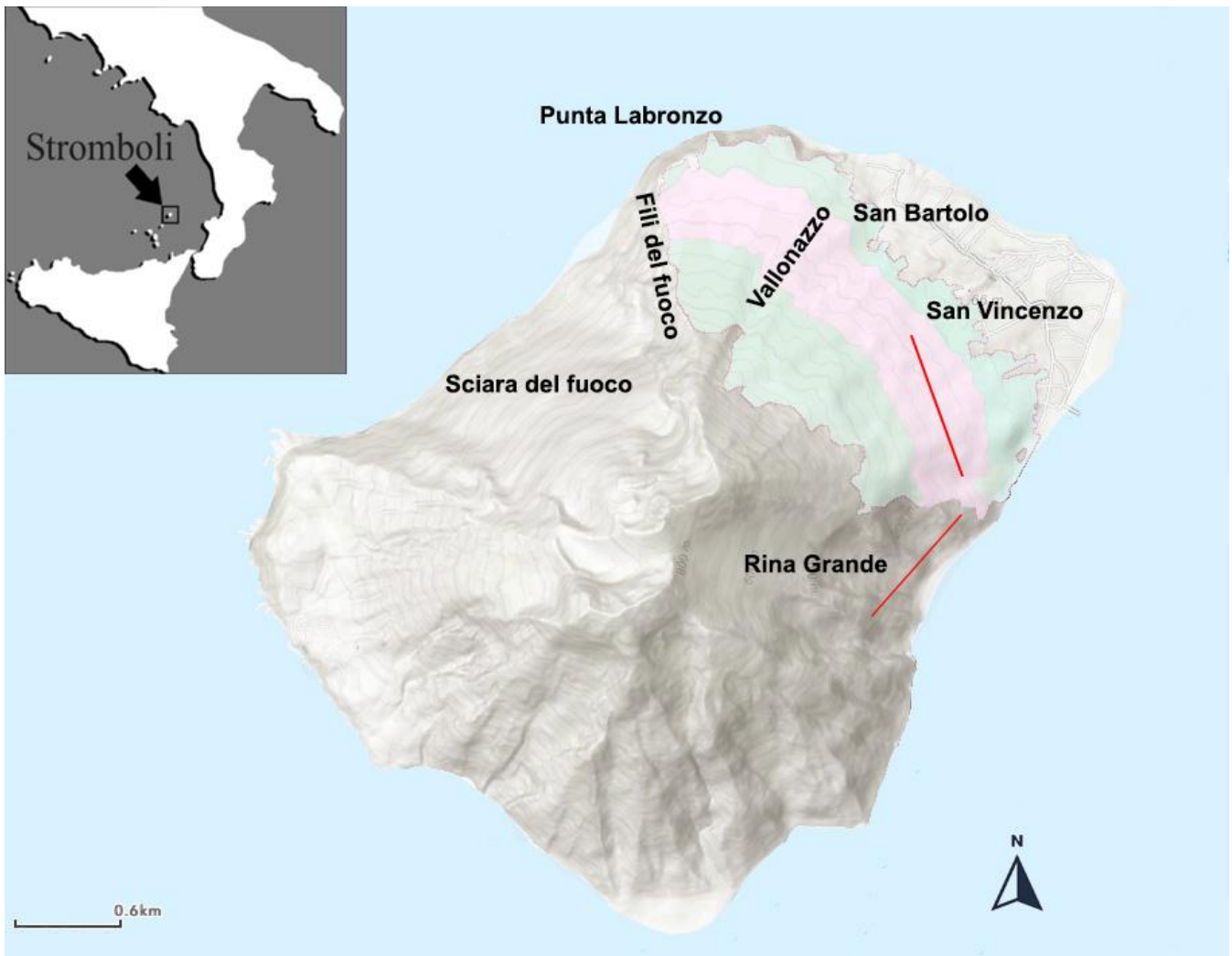
533 Vallejo, V. R., Allen, E. B., Aronson, J., Pausas, J. G., Cortina, J., and Gutiérrez, J. R.: Restoration of Mediterranean-type
534 woodlands and shrublands, in: *Restoration Ecology: The New Frontier*, edited by Andel, J. and Aronson, J. (Eds.), Blackwell
535 Publishing Ltd.: Oxford, UK, 130–144, 2012.

536 Weiser F., Sauer A., Gettueva D., Field R., Irl S.D.H., Vetaas O., Chiarucci A., Hoffmann S., Fernández-Palacios J.M., Otto
537 R., Jentsch, A., Provenzale, A. and Beierkuhnlein, C.: Impacts of forest fire on understory species diversity in Canary pine
538 ecosystems on the island of La Palma. *Forests*, 12(12), 1638, 2021.

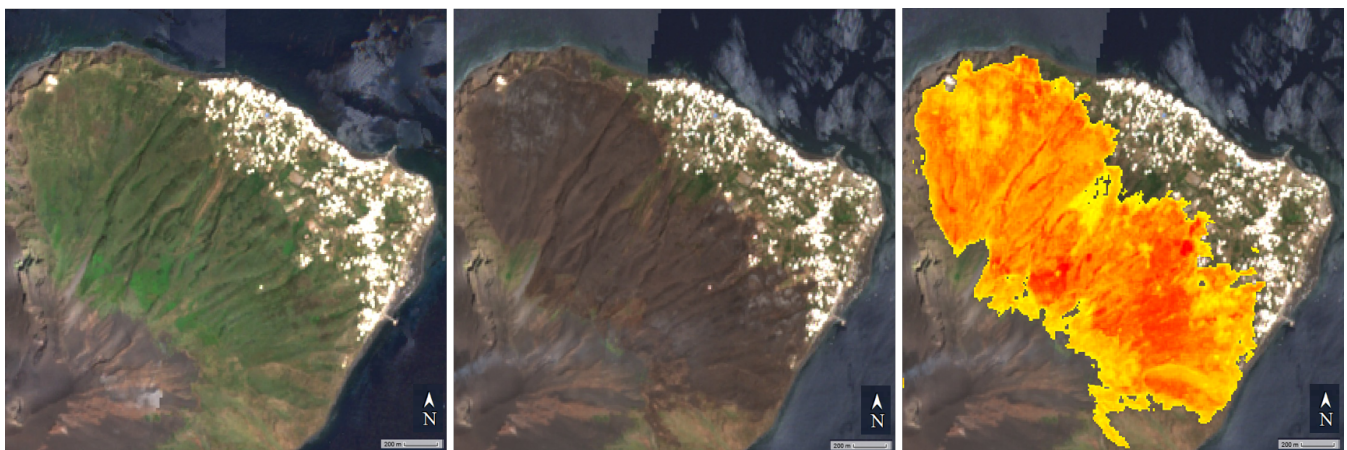
539 Zaia, R., Pasta, S., Di Rita, F., Laudicina, V. A., Lo Cascio, P., Magri, D., Troia A., and Guarino, R.: Staying alive on an active
540 volcano: 80 years population dynamics of *Cytisus aeolicus* (*Fabaceae*) from Stromboli (Aeolian Islands, Italy), *Ecological*
541 *Processes*, 9(1), 1–15, <https://doi.org/10.1186/s13717-020-00262-5>, 2020.

542 Hearst, Marti A., et al. "Support vector machines." *IEEE Intelligent Systems and their applications* 13.4 (1998): 18-28.

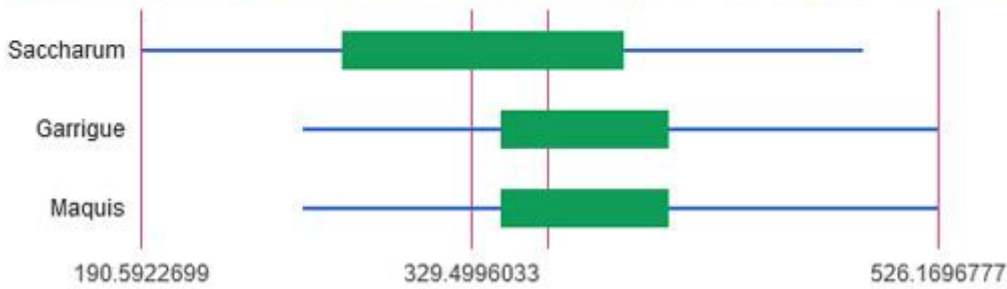
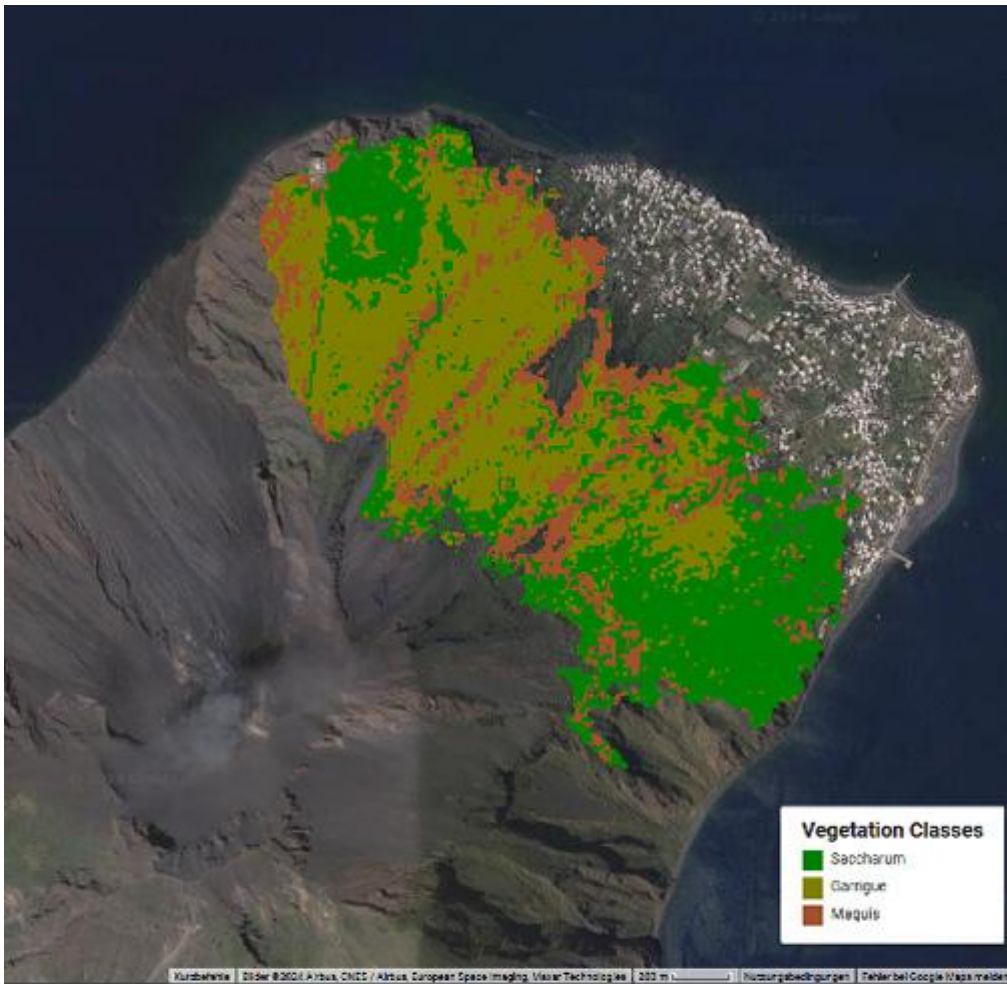
543



544
 545 **Figure 1:** Map of the study area (light green) with the place names mentioned in the text. The pink colour indicates the area where
 546 the vegetation plots for validation were sampled. Red lines identify the two transects along which the stem density of *Saccharum*
 547 was measured.



551
 552 **Figure 2:** (from left to right) Sentinel 2 image before fire event (composite of acquisitions in the time period 22/04 - 22/05/2022);
 553 Sentinel 2 image after fire (composite of acquisitions in the time period 25/05/22-15/06/2022); *dNBR*-inferred burned area (yellow:
 554 low-, orange: middle-, red: high-severity damage) overlaid on the middle image composite.



556

557

558

559

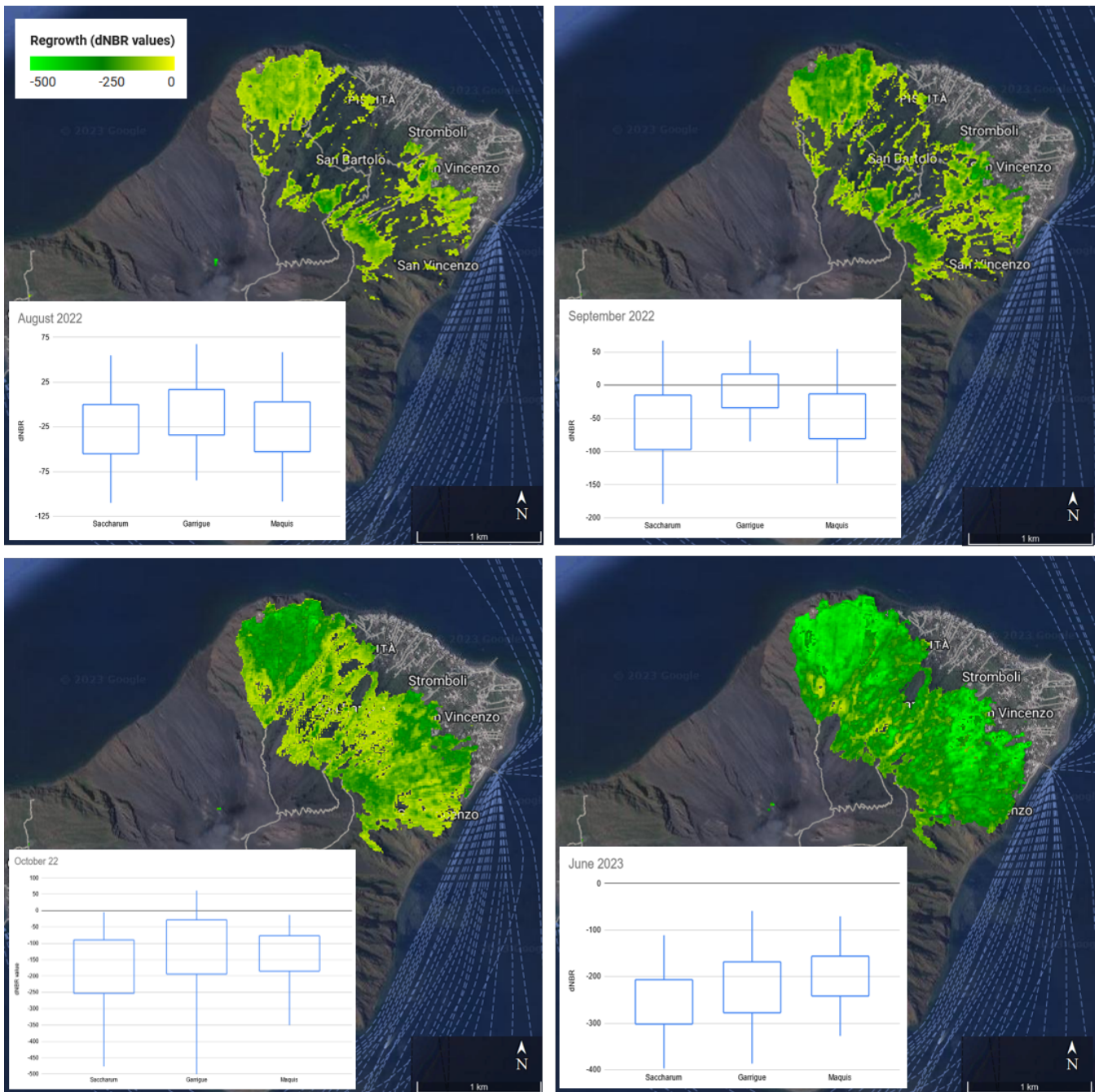
560

561

Figure 3: (top) supervised classification of vegetation classes in the study area, overlaid on Google Earth base map (© 2024 Airbus, CNES/Airbus, European Space Imaging, Maxar Technologies); (bottom) Boxplot showing the distribution of $dNBR$ values per vegetation class, evaluated on the image composites from acquisitions in the periods 15 April - 22 May and 26 May -15 June 2022. Boxes and whiskers correspond to one and two standard deviations, accounting for 68% and 95% of the processed values, respectively. Fire occurred in garrigue and maquis was estimated to be the most severe.

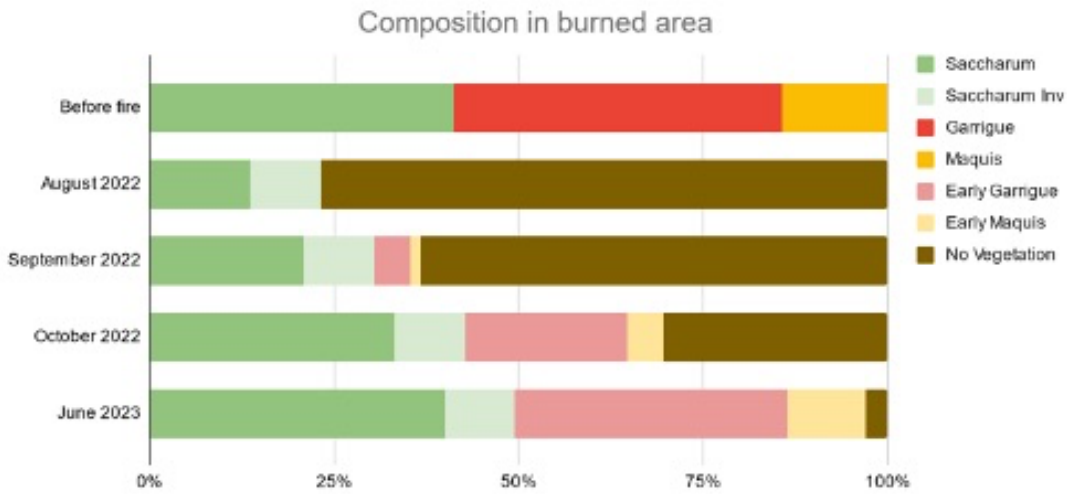


562
563
564
565
566
567
568
569
570
571
Figure 4: (left) high resolution drone image acquired on 17 August 2022 to assess the quality of the information derived from *dNBR* analysis, overlaid on an high resolution image from Google Earth basemap; (top right) pre-fire detail from Google Earth basemap; (middle right) post-fire detail from drone image; (bottom right) same detail with overlaid thresholded *dNBR* values higher than 0.19 (using pre-fire and August 2022 scene), semitransparent for visual comparison (yellow: low-, orange: middle-, red: high- severity damage). Credits of drone images: Antonio Zimbone. Credits for Google base map: © 2024 Airbus, CNES/Airbus, European Space Imaging, Maxar Technologies.



572
 573
 574
 575
 576
 577
 578
 579
 580

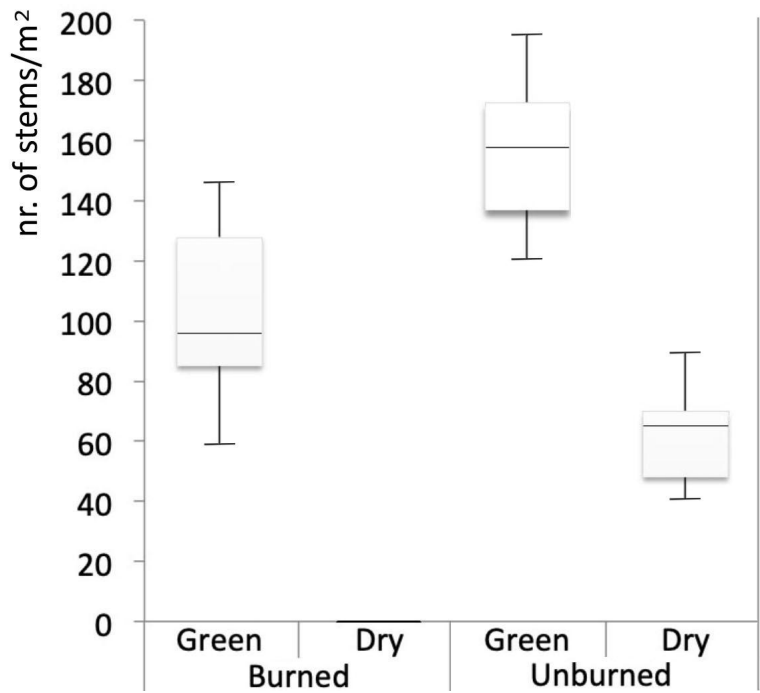
Figure 5: Vegetation recovery in the area affected by the fire, estimated through dNBR values from different acquisitions of Sentinel-2 images, overlaid on Google Earth base map (© 2024 Airbus, CNES/Airbus, European Space Imaging, Maxar Technologies). Boxplots show the distribution of dNBR values associated with recovery in the areas occupied by Saccharum, garrigue, and maquis. Boxes and whiskers correspond to one and two standard deviations, accounting for 68% and 95% of the processed values, respectively. The following thresholds were suggested by Key and Benson (1996) to categorise levels of recovery from dNBR values rescaled by 1000: no change from 0 to -100, low enhanced recovery from -100 to -250, and high enhanced recovery (high) from -250. *Saccharum* is characterized by faster recovery than the maquis and the garrigue, particularly at the beginning of the first growing season after fire (September-October 2022).



581
582
583
584
585
586

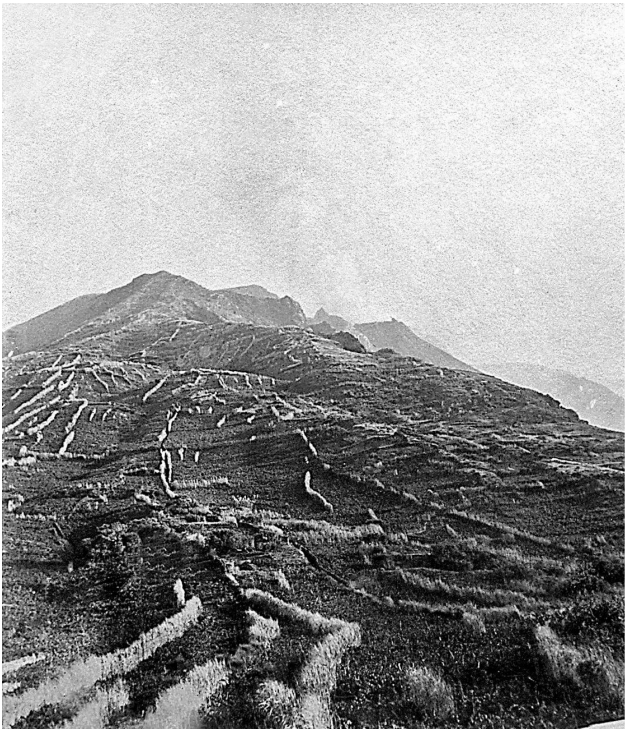
Figure 6: estimated vegetation composition in the study area (cover %). "Saccharum" vegetation patches occupied by Saccharum both before and after fire; "Saccharum Inv" sums the surface areas previously occupied by other vegetation units and invaded by Saccharum after fire. "Early garrigue" and "Early maquis" refer to early post-fire successional stages of these two vegetation classes, dominated by annual plants, resprouted shrubs and seedlings of perennial seeders, chiefly *Cistus sp. pl.*

587
588



589
590
591

Figure 7: (left) measuring resprouted *Saccharum biflorum* stem density in one of the plots within the burned area (18 Sept. 2022, photo by R. Guarino); (right) boxplots of the stem density of *Saccharum* in burned and unburned patches.



592
593
594

Figure 8: (left) historical photo of terraced vineyards on Stromboli (year: 1891, anonymous), with rows of *Saccharum biflorum* used as windbreaks; (right) same view, 130 years later (16 July 2021, photo by P. Lo Cascio).